The 5th IEEE International Conference on E-Health and Bioengineering - EHB 2015
Grigore T. Popa University of Medicine and Pharmacy, Iaşi, Romania, November 19-21, 2015

Unsupervised Detection and Classification of Motor Unit Action Potentials in Intramuscular Electromyography Signals

Hooman Sedghamiz, Daniele Santonocito
MED-EL GmbH, Innsbruck, Austria, {Hooman.Sedghamiz, Daniele.Santonocito}@medel.com

***Abstract*— A computationally efficient and unsupervised algorithm for the detection and clustering of motor unit action potentials (MUAPs) recorded in a single-channel Intramuscular Electromyography (EMG) is presented. The detection of MUAPs is performed with a modified version of the multiresolution Teager energy operator (MTEO). The unsupervised clustering of action potentials is achieved by applying a combination of label and template matching techniques. The proposed algorithm reduces the partial superimposition of MUAPs with a new MTEO based analysis method. The computational speed of the method is also improved by using the principal component analysis (PCA) in order to reduce the number of templates and fiducial point detection and consequently to decrease the correlation computation load. The performance of the algorithm is examined on several intramuscular EMG recordings of different healthy and diseased muscles such as the posterior cricoarytenoid and tibiliasis anterior.**

Keywords—electromyography; template matching; unsupervised classification; decomposition.

I. INTRODUCTION

Intramuscular EMG is the recording of the electrical excitation related to the muscle fibers in the motor units (MUs) by inserting needles or wires [1]. Each MU contains an ensemble of motoneurons (MNs) that generate pulse trains known as action potentials (APs). The sum of APs forms the so called motor unit action potential (MUAP) [2]. The analysis of MUAPs morphology can assist in the diagnosis of myopathies and other diseases associated with the neuromuscular junction. However, manual decomposition of MUAPs is a hard and time consuming task. Therefore researchers have focused on developing algorithms that are able to automatically detect and isolate MUAPs [1]. Several algorithms have been proposed for the EMG decomposition task. Some algorithms are fast [3], [4], but unable to reduce superimpositions and interferences and therefore they suffer from low accuracy. Other algorithms such as the work described by LeFever and Deluca [5] are accurate but computationally heavy and hence slow and not suitable for long recordings. On the other hand, the Montreal EMG decomposition (MTLEMG) proposed by Florestal, Mathieu and Malanda [2], achieves an acceptable tradeoff between speed and accuracy by combining label and template matching techniques. However, the method is not suitable for the noisy EMG measurements due to the detection strategy employed.

The identification of individual MUAPs in an intramuscular EMG recording consists of two main stages: detection and classification. In the detection phase, the goal is to differentiate MUAPs from noise. In the classification stage, the detected MUAPs are assigned to a cluster based on their morphology. The aim of this paper is to improve the detection accuracy and enhance the computational speed of classification while preserving the reliability of the decomposition. A multiresolution Teager energy operator (MTEO) [6] along with a statistical analysis [7] are employed in the detection stage, which simultaneously tests both the instantaneous frequency and amplitude of the MUAPs in order to reduce the false detections and improve the detection accuracy. In the classification stage, the MTEO output is used for the MUAPs alignment, templates reduction and feature extraction so as to reduce the background noise and unrelated spikes. Finally, Label and template matching techniques similar to MTLEMG [2] are used in order to improve both the speed and clustering sensitivity of the algorithm.

II. METHODS

A. MUAP Detection

The first step of the algorithm is to detect the initial set of MUAPs in the noisy EMG recording. The detection module consists of the *signal enhancement*, *MTEO computation*, and *Statistical Thresholding*.

1) Signal Enhancement: First, a narrow notch filter is applied to remove the 60 Hz power-line noise. Then, the signal is normalized to the unit variance and de-trended, i.e. linear trends are removed from the signal. Finally, a band-pass fourth order Butterworth filter (5-1200 Hz) is employed to reduce the interfering noise in the signal.

2) MTEO Computation: MUAPs have typically high amplitude and instantaneous frequency. The Teager energy operator (TEO) is a time-frequency analysis and has been employed in many different signal processing applications [6]. Its general form is defined as,

$$\varphi\{x(nT)\} = x^2(nT) - x(nT - T)x(nT + T) \quad (1)$$

K-TEO is a multi-resolution version of TEO in which $x(nT - T)x(nT + T)$ is replaced by $x(nT - kT)x(nT + kT)$, where k is an arbitrary integer called the *lag parameter* and T is the sampling rate. Therefore, TEO can be tuned in order to be sensitive to more specific frequencies. K-TEO is an attractive tool due to its low computational power and effectiveness compared to the other time-frequency approaches such as the continuous wavelet transform (CWT). The MTEO approach used in this paper is similar to the work by Choi, Jung and Kim [6].

Let $x(nT)$ be the raw EMG signal for $n = 1, 2, \dots N$, where N is the number of signal samples. The K-TEO is defined as,

$$Y_k(nT) = x^2(nT) - x(nT - kT)x(nT + kT) \quad (2)$$

where the choice of *k* is based on the *period* of the spike that is being searched for. In fact increasing *k* makes the detector less sensitive to the higher frequencies and more sensitive to the lower frequencies. The final output of MTEO $t(nT)$ is computed as,

$$t(nT) = \max\{\widehat{Y_1}(nT), \widehat{Y_2}(nT), \dots, \widehat{Y_k}(nT)\} \quad (3)$$

where $\widehat{Y_k}(nT)$ is $Y_k(nT)$ after it is smoothed with a Hamming window of size *4k+1* and normalized by the squared variance at scale *k*. Fig. 1 shows a segment of an EMG recording processed at three *k* levels and the final MTEO output.

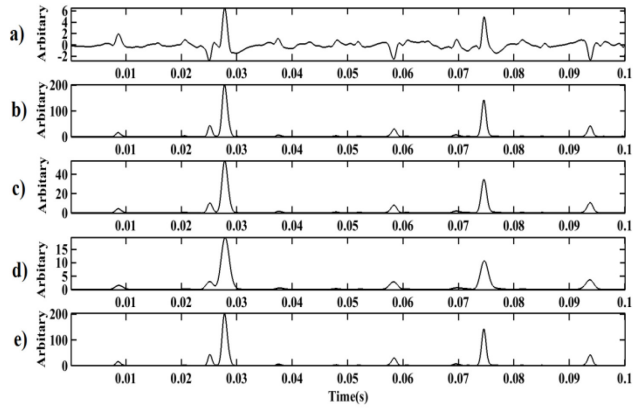

Fig. 1. (a) Band-pass filtered and normalized EMG signal. (b), (c) and (d) Outputs of k-TEO at *k = 2, 3* and 5 respectively. (e) The output of MTEO after passing all the scales through a maximum energy detector.

3) Statistical Thresholding: The aim of this stage is to determine the arrival time of MUAPs in $t(nT)$. Here we employ a statistical testing similar to the method mentioned in Nenadic et al [7]. First, two binary hypothesis states are defined as $H_0$when the MUAP is not present, and $H_1$when both the MUAP and noise are present:

$$H_0: t(nT) = G(nT) \quad (4)$$
$$H_1: t(nT) = s(nT) + G(nT) \quad (5)$$

$s(nT)$ is the MUAP signal and $G(nT)$ is a random Gaussian noise sequence. Since the median of a random variable is less sensitive to outliers than its variance, the standard deviation of $t(nT)$ can be approximated as the median of its absolute deviation [7],

$$\hat{\sigma} = MEDIAN\{|t(T) - \mu|, \dots, |t(NT) - \mu|\}/0.6745 \quad (6)$$

where μ is the sample mean. In the next step, for a near optimal performance a threshold TH_1 is chosen as:

$$TH_1 = \hat{\sigma}\sqrt{2\log_e N} \quad (7)$$

Hence, $t(nT)$ is compared to TH_1 and divided into noisy segments $t^G(nT)$ and signal segments $t^S(nT)$:

$$t^G(nT) \triangleq \{t(nT) \leq TH_1\} \quad (8)$$

$$t^S(nT) \triangleq t(nT) \backslash t^G(nT) \quad (9)$$

The prior probabilities of the two binary hypothesis, $P(H_0)$ and $P(H_1)$ are estimated as the size of $t^G(nT)$, and $t^S(nT)$ respectively:

$$P(H_0) = ||(t^G(n))||/N \quad (10)$$
$$P(H_1) = ||(t^S(n))||/N$$

where $||.||$ stands for the size.
Consequently, the final decision rule threshold TH_2 is formulated as,

$$TH_2 = \frac{\mathfrak{m}}{2} + \frac{\hat{\sigma}^2}{\mathfrak{m}}\left(C + \log_e \frac{P(H_0)}{P(H_1)}\right) \quad (11)$$

where $\mathfrak{m}$ is the sample mean of the absolute value of $t(n)$ under the hypothesis H_1, and C is a scaling constant selected by the user that determines the sensitivity of the detection. After testing $t(nT)$ against TH_2, a signal containing the MUAP samples is generated:

$$MU(nT) \triangleq \{\mathrm{t(nT)} \geq TH_2\} \quad (12)$$

The final output of the MUAP detection algorithm is a set of the local maxima indices $D = \{d_1, d_2, \dots, d_m\}$ in $MU(nT)$ which are at least 1ms apart. Extracting these fiducial points highly enhances the speed of the template matching procedure.

B. MUAP Classification

The task of the MUAPs classification is divided into the following stages: *Windowing, Interference Cancelation, Alignment, Template Reduction, Labeling, Merging* and *Assigning MUAPs.*

1) Windowing: MUAP segments are extracted from both the filtered EMG, $x(nT)$ and the output of MTEO, $t(nT)$. For each d_i in the vector D obtained from the previous stage, a window with a fixed length (~20 ms) is centered at d_i, in order to extract a pair of segments X_i and T_i from $x(nT)$ and $t(nT)$ respectively. Therefore, two matrices each containing m segments with fixed lengths are formed:

$$X = \{X_1, X_2, \dots, X_m\}.$$
$$T = \{T_1, T_2, \dots, T_m\}.$$

2) Interference Cancelation: The extracted segments from the windowing section might contain residuals from the neighboring MUAPs which result in being partially or completely superimposed. Two partially superimposed MUAPs appear, in the output of the MTEO, as two dominant maxima and a single minimum in between separating them. In order to cancel out such interferences, a threshold TH_{int} is computed by weighting TH_2 which was previously calculated from Eq. (11),

$$TH_{int} = \omega TH_2 \tag{13}$$

where $\omega \in [0,1]$ is a weighting factor. Since the output of MTEO generates clear valleys at the locations where both the amplitude and instantaneous frequency of the signal damp [Fig. 2(b)], it is used to split such interferences. First, all of the extrema in the segment T_i are detected. We denote the indices of the local maxima as $MI_i = \{b_{1i}, \dots, b_{Ei}\}$ and the amplitude of the corresponding maxima as $MA_i = \{a_{1i}, \dots, a_{Ei}\}$, where E_i is the total number of maxima in T_i. Similarly, $MN_i = \{b_{1i}, \dots, b_{Oi}\}$ and $ML_i = \{a_{1i}, \dots, a_{Oi}\}$ contain the indices and amplitudes of the local minima in T_i respectively. The proposed method checks whether a maximum is exceeding TH_{int} and is also followed by a local minimum that falls below the sample mean μ of $t(nT)$. If such a condition is met, zero padding in the segments T_i and X_i is applied from the corresponding index of the local maximum b_{E_i} till the index b_{O_i} of the local minimum after/before it. Formally, the following conditions are checked for each half of the segment T_i,

$$\begin{cases} (a_{Ei} \geq TH_{int}) \wedge (a_{Oi} \leq \mu) \wedge (b_{E_i} < b_{O_i}) \wedge (abs(b_{E_i} - \frac{L}{2}) > \varepsilon) \wedge (E_i, O_i) < \frac{L}{2} \\ (a_{Ei} \geq TH_{int}) \wedge (a_{Oi} \leq \mu) \wedge (b_{E_i} > b_{O_i}) \wedge (abs(b_{E_i} - \frac{L}{2}) > \varepsilon) \wedge (E_i, O_i) \geq \frac{L}{2} \end{cases}$$

where L is the length of T_i (~20 ms) and ε is a small tolerance distance value that avoids the splitting of the very compact MUAPs.

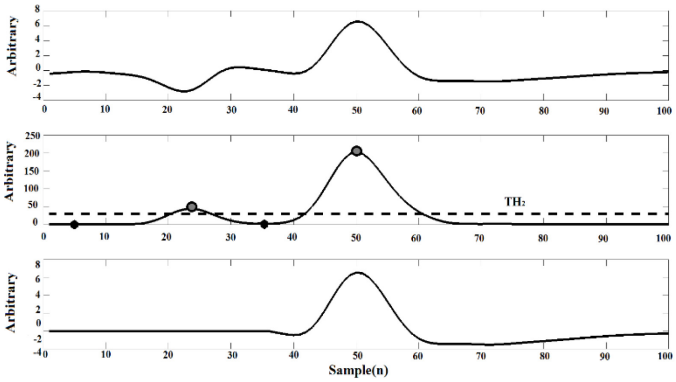

Fig. 2. Illustration of the interference cancelation. (a) Two MUAPs which are partially superimposed (b) Output of the MTEO which shows a clear *valley* (denoted by diamonds) in between the two maxima (denoted by circles). The dotted line indicates the level of TH_{int}. (c) Interference free version of (a) by zero padding the part containing the superimposition.

2) Alignment: There are several different algorithms for the MUAP alignment such as the threshold crossing and global maxima detection based methods. However, the performance of these approaches degrades as the SNR of the signal decreases. We have utilized the output of MTEO for this task since it is less sensitive to the background noise. The alignment is performed in a two stage method similar to the approach proposed by Choi et al. [6]. First, the global maximum in segment T_i is used in order to align the MUAPs. Then the closest extremum in X_i to the global maximum in T_i is employed to fine tune the alignment.

3) Template reduction and Labeling: Principal Component Analysis (PCA) is a statistical approach employed to reduce the dimensionality of datasets [8]. PCA computes $RP = P\Gamma$, where R is the covariance matrix of a multivariate dataset such as X in this work, P is the eigenvector and Γ is the eigenvalue matrix. The PCA is applied on the signal X which contains the patterns, and then the computed eigenvalues are compared against a tolerance value ς. If the eigenvalue of a principal component (PC) is lower than this value, then the PC corresponding to that particular pattern is set to zero.

In the next step, a symbolic representation of the patterns is used since it highly enhances the speed of clustering [2]. Four features are extracted from each template in T_i and X_i as illustrated in Fig. 3. For the feature selection task, we use both the template outputs of MTEO and the band-passed filtered EMG signal in order to have a more comprehensive representation. The first feature is the number of extrema in the template T_i that exceed the threshold TH_2. For instance in Fig. 3(a) two extrema are detected in T_i. Fig. 3(b) shows how the extrema of T_i interpreted from the extrema in X_i: the first extremum represents a local maximum, whereas the second is a local minimum.

Local minima and maxima are labeled with the digit 1 and 2 respectively. The second feature is the approximate period

of each peak in T_i and a rectangle symbol is used to denote it in Fig. 3(a). The period is computed as the number of samples between the two local minima that are preceding and following the detected peak respectively and that are lower than μ. Fig. 3(a) shows three vertical lines in correspondence of the local minima matching the mentioned criteria and finally used for the approximate period computation. The third and fourth features are the amplitude and phase of the extrema in T_i and are denoted with a hexagon and circle symbols respectively in Fig. 3(a). The numerical value of features 2, 3 and 4 are linearly mapped to an integer ranging from 1 to 9 in order to generate consistent labels. Consequently, each template is assigned with four labels. For instance in Fig. 3, the labels are "21", "23'',''15'' and "43" respectively. The templates having four identical labels or labels that differ by no more than one digit in the 2nd, 3rd or 4th features are grouped together. For instance, a template with labels "21", "23'', "43" and ''15'' will be grouped with a template having the labels "21", "33'', "43" and ''15'', but not with "22", "43'', "43" and ''15'', since the two templates have different labels for the first feature.

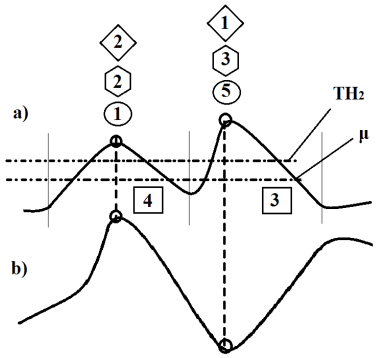

Fig. 3. An example of feature selection approach is shown. (a) Template T_i contains two extremum that cross TH_2 and are separated by a minimum that is lower than μ. (b) The same template from the band-pass filtered signal X_i is shown. The first extremum in T_i is a local maximum for X_i (denoted by diamond 2) whereas the second is a minimum (denoted by diamond 1). The other features are first mapped to an integer between 1 to 9 and then assigned to the peaks. For instance, the approximated period of the first extremum is mapped to 4 and the second to 5. In this way, each pattern has four labels and a simple label matching technique can be used to identify similar patterns.

2) Merging: In order to merge the clusters that are similar but not grouped together in the previous state, as well as the inter-cluster homogeneity, a template matching approach known as *pseudocorrelation* (PsC) is employed. It has been shown in [2] that PsC is a more sensitive measure of similarity between two patterns than the standard cross-correlation approaches. Therefore, we have used PsC as a measure of similarity analysis in this work. Based on [2], PsC is formulated as,

$$PsC_z = max\left\{\frac{\sum_{j=1}^{m}\left(v_j y_{z+j} - |v_j - y_{z+j}|\max\{|v_j|,|y_{z+j}|\}\right)}{\sum_{j=1}^{m}\left(\max\{|v_j|,|y_{z+j}|\}\right)^2}, 0\right\} \quad z = 1,2,\dots,f \tag{14}$$

where v is the template with length m in the sequence y with length f ($m \leq f$).

First, a template is generated from each cluster formed in the labeling step by computing the median of its members, since median is less sensitive to outliers. To ensure the inter-cluster homogeneity, the similarity of each member of the cluster to the template is computed with PsC. The members that have a similarity lower than a threshold Q are removed from that cluster and a new template is generated by computing the median of the remaining members.

In order to check the similarity between two specific clusters, the PsC score is calculated between their corresponding templates. If the PsC is higher than Q, the two corresponding clusters are merged. Finally, those clusters having a few members in respect to the length of the signal and irregular firing patterns are also removed.

Assigning MUAPs: This step assigns each MUAP in the band-pass filtered signal $x(nT)$ to a specific template generated in the previous steps. In order to avoid a sample by sample PsC computation that would become a function of the length of $x(nT)$, we have used the fiducial indices $D = \{d_1, d_2, \dots, d_m\}$ computed in the detection stage of the algorithm. PsC is calculated by slightly shifting the template around these indices and the highest PsC score is stored. If the corresponding PsC score is higher than the threshold Q, the MUAP is assigned to that template and the matching part is subtracted from the signal $x(nT)$. This approach is known as Peel-off detection [1].

C. Implementation

The proposed algorithm is implemented in Matlab and C in the form of a standalone computer program. The parameters of the algorithm such as C and Q are tuned from the visual interface of the software. The software also provides some other features such as synchronized plug and play of the channels. The program also outputs some statistics about the firing patterns and the total number of turns in the signal. Furthermore, an optimization approach is implemented in the software that automatically estimates the values for C and Q based on the input EMG signal. The complete steps of the proposed algorithm are detailed in Fig. 4.

III. RESULTS

In order to evaluate the accuracy and computational speed of the proposed algorithm, several EMG recordings from posterior cricoarytenoid, tibiliasis anterior and brachial bicep muscles are employed. The recording from the posterior cricoarytenoid muscle is 2.5 seconds long, sampled at 10 kHz and contains 3 unique MUAP templates. Fig. 5 shows the test signal 1 and a zoomed-in segment labeled with our proposed algorithm. The Two other recordings belong to the tibiliasis anterior muscle, are sampled at 4 kHz and one of them is from a subject suffering from myopathy [9]. We have included diseased muscles in the analysis in order to evaluate the performance of the algorithm in detecting the poly-phasic

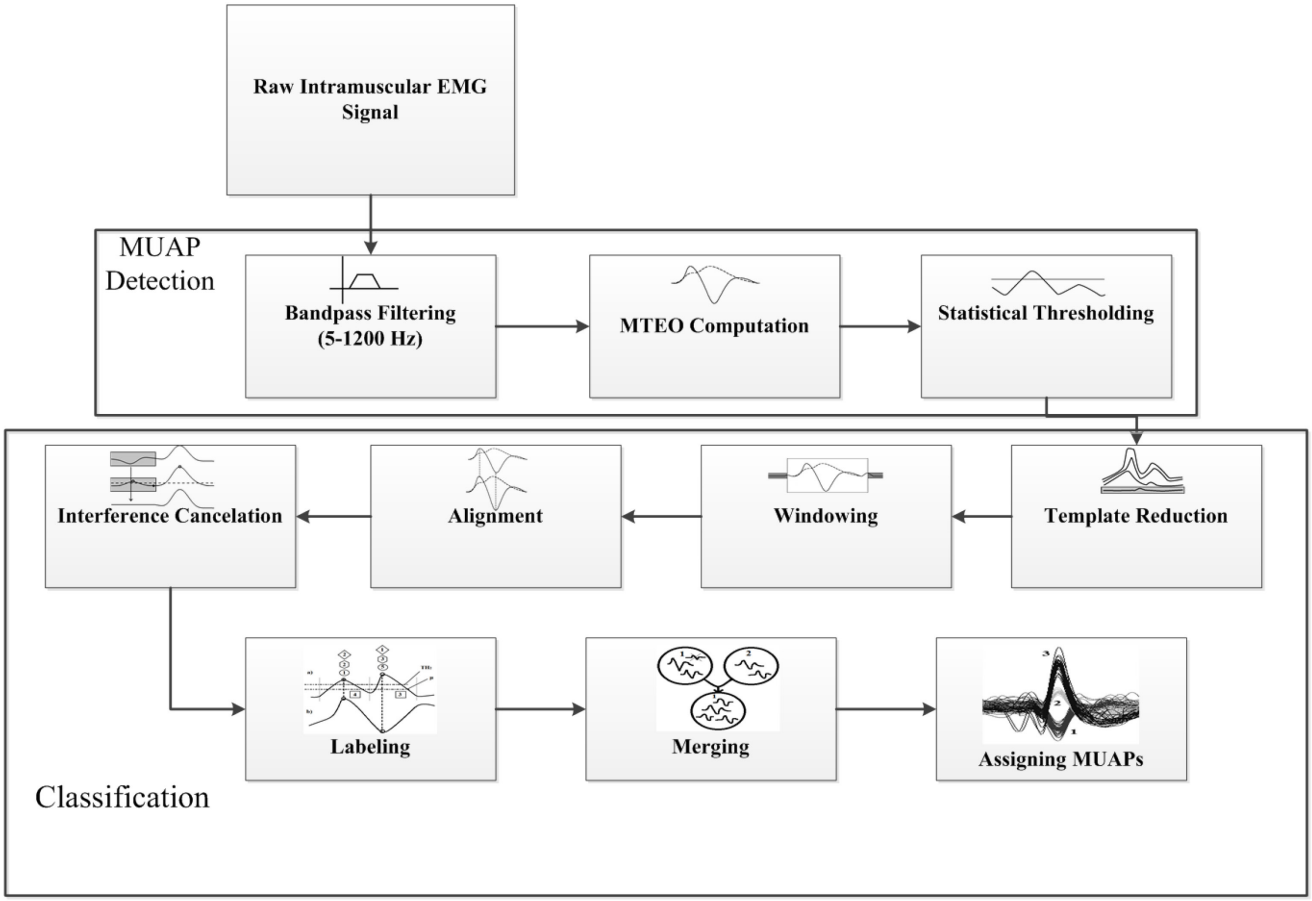

Fig. 4. The detailed steps of the proposed algorithm. The main blocks of the algorithm are MUAP Detection and Classification.

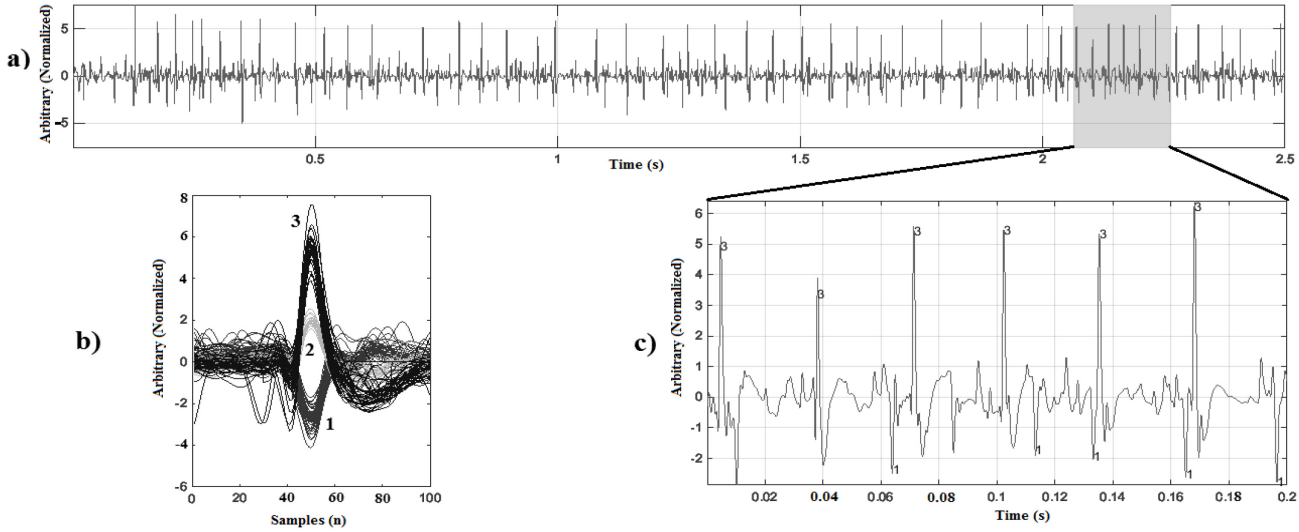

Fig. 5. The output of the software is shown after applying the algorithm on a 2.5 second test EMG signal from the Posterior Cricoarytenoid muscle. (a) Raw band-passed filtered and normalized EMG signal. (b) Unsupervised detected templates. Three unique templates are identified. (c) A zoomed in view of the labeled MUAPs in the software.

and deformed MUAPs. The last recording is from the brachial bicep and contains 8 unique MUAP trains [10]. In order to assess the accuracy of the method, first, we calculated the sensitivity $Se_{Overal} = TP_{Overal}/(TP_{Overal} + FN_{Overal})$ and $P_{Overal} = TP_{Overal}/(TP_{Overal} + FP_{Overal})$ in the templates level representing the ability of the algorithm in extracting the main unique templates in each recording. In the second step, we computed Se_{Temp_i} and P_{Temp_i} for the correctly detected template i. For instance, if a template is correctly identified, we count how many MUAPS in the signal are clustered under this template. These parameters represent the *homogeneity* in the template i cluster. From Se_{Temp_i} and P_{Temp_i}, we computed $Se_{Temp_{avg}} = 1/n \sum_1^n Se_{Temp_i}$, and $P_{Temp_{avg}} =$

Recordings	Nr. MUAP Temp*	Method	Se_{Overal} (%)	P_{Overal} (%)	$Se_{Temp_{avg}}$ (%)	$P_{Temp_{avg}}$ (%)	Computational Time (s)
Sig 1: Posterior Cricoarytenoid	3	This work with Inter. Canc **	100	100	90.82	100	0.848
		This work without Inter.Canc	100	100	83.05	100	0.819
		MTLEMG [2]	66	100	39.43	83	1.201
Sig 2: Tibiliasis Anterior with myopathy	4	This work with Inter. Canc	75	100	92.22	95.43	7.421
		MTLEMG [2]	66	33	53.55	59.65	53.201
Sig 3: Tibiliasis Anterior healthy	7	This work with Inter. Canc	71.73	100	N/D***	N/D	1.990
		MTLEMG [2]	100	77.7	N/D	N/D	4.692
Sig 4: Brachial Bicep	8	This work with Inter. Canc	62.5	71.4	N/D	N/D	2.021
		MTLEMG [2]	100	88.8	N/D	N/D	3.702

Table 1. Algorithm accuracy and computational time

* Number of unique MUAP templates manually determined
** Interference Cancelation used with the algorithm
*** Not Determined (N/D)

$1/n \sum_1^n Se_{Temp_i}$, where n is the total number of correctly identified templates in order to achieve global values. However, due to the high complexity of the signals, we could determine $Se_{Temp_{avg}}$ and $P_{Temp_{avg}}$ just for signals 1 and 2 in Table 1, since the number of superimpositions in the last two recordings made it very difficult to confidently determine the precise number of MUAPs belonging to each template. The 4 recordings used in this study contained a total of 22 unique templates (3, 4, 7 and 8 respectively). We could manually count a total number of 266 (i.e. 55 + 51 + 47 + 65 + 48) MUAPS for 5 of these templates in the first and second recordings. Table 1 summarizes these results. One of the few unsupervised algorithms that is able to decompose the EMG signals without major parameter tuning is MTLEMG [2]. Therefore, we compared the accuracy and computational time required for processing the test signals with this method. Signal 1 contained 3 unique templates each containing 55, 25 and 47 MUAPs. Our algorithm was able to correctly identify all the 3 templates ($Se_{Overal} = 100\%, P_{Overal} = 100\%$). Our method assigned 51, 21 and 45 MUAPs to templates 1, 2 and 3 respectively, resulting in a high sensitivity rate ($Se_{Temp_{avg}} = 90.82\% = 1/3 \sum_1^3 Se_{Temp_i} = 1/3[92.73 + 84 + 95]$). As the test signals became more complex (e.g. signals 3 and 4), the overall performance of MTLEMG improved and the performance of our method degraded. This is due to the increased levels of superimpositions.

IV. Discussion and Conclusions

The proposed algorithm achieves a fast processing speed by using a fiducial point detection technique instead of processing the complete signal in the template matching stage. The MTEO accompanied by the statistical analysis approach introduced in this work, increases the sensitivity of the algorithm by resolving the partial superimpositions. The PCA removes the extracted redundant templates before the labeling stage. Templates are also represented in a more comprehensive way by employing both the MTEO output and the band-pass filtered signal, which in turn improve the reliability of the classification. The current algorithm is able to resolve partial superimpositions with a MTEO and peel-off detection method. However, in order to resolve complete superimpositions, a different approach is required, since it is not possible to resolve the complete superimpositions with the above mentioned methods.

References

[1] J.R. Merletti, and D. Farina, "Analysis of intramuscular electromyogram signals," *Phil. Trans. Roy. Soc. London,* pp. 357-368, November 2008.

[2] J.R. Florestal, P.A. Mathieu, and A. Malanda, "Automated Decomposition of Intramuscular Electromyographic Signals," *IEEE. Trans. Biomed. Eng.,* vol. 53, NO. 5, May. 2006.

[3] D. Stashuk, H. DeBruin, "Automated Decomposition of selective needle-detected myoelectric signals," *IEEE. Trans. Biomed. Eng.,* vol. 35, pp. 1-10, Jan. 1988.

[4] K.C. McGill, K.L Cummins, and L.J.Dorfman, "Automatic Decomposition of the clinical electromyogram," *IEEE. Trans. Biomed. Eng.,* BME-22, pp. 470-476, 1985.

[5] R.S. LeFever and C.J. Deluca, "A procedure for decomposing the myoelectric signal into its constituent action potentials-Part I: technique, theory and implementation," *IEEE. Trans. Biomed. Eng.,* vol. BME-29, pp. 149-257, 1982.

[6] J.H. Choi, H.K. Jung, and T. Kim, "A New Action Potential Detector Using the MTEO and Its Effects on Spike Sorting Systems at Low Signal-to-Noise Ratios," *IEEE. Trans. Biomed. Eng.,* vol. 53, NO. 4, pp. 738-746, April 2006.

[7] Z. Nenadic and J.W. Burdick, "Spike Detection Using the Continuous Wavelet Transform," *IEEE. Trans. Biomed. Eng.,* vol. 52, pp. 74-87, Jan. 2005.

[8] I.T. Jolliffe, Principal Component Analysis, Series: Springer Series in Statistics, 2nd ed., Springer. NY, 2002 pp. 487.

[9] J. Kimura, Electrodiagnosis in Diseases of Nerve and Muscle: Principles and Practice, 3rd Ed. New York, Oxford University Press, 2001.

[10] K.C. McGill, [Online dataset R001, available at http://www.emglab.net]